Perfusion of the interventricular septum during ventilation with positive end-expiratory pressure

BERNHARD ZWISSLER, MD; RUDOLF SCHOSSER, MD; CHRISTIANE SCHWICKERT; PETER SPENGLER; MICHAELA WEISS; VOLKER IBER; KONRAD MESSMER, MD

Objective: **To determine whether regional hypoperfusion of the interventricular septum occurs during ventilation with positive end-expiratory pressure.**

Design: **Animal study.**

Animals: **Anesthetized, closed chest dogs (n = 8).**

Interventions: **Induction of experimental adult respiratory distress syndrome (ARDS) and then ventilation with 10, 15, and 20 cm H_2O of positive end-expiratory pressure.**

Measurements and Main Results: **Cardiac output and regional interventricular septum blood flow were assessed at control, at induction of experimental ARDS, and at each level of positive end-expiratory pressure. Ventilation with 20 cm H_2O of positive end-expiratory pressure decreased cardiac output (–32% vs. control, $p < .05$), and did not change absolute, but increased relative (to cardiac output) interventricular septum blood flow. During experimental ARDS and ventilation at 20 cm H_2O end-expiratory pressure, there was a redistribution of flow toward the right ventricular free wall (+93%, $p < .001$) and the right ventricular part of the interventricular septum (+68%, $p < .01$), while flow to the left ventricular interventricular septum and to the left ventricular free wall remained unchanged. Locally hypoperfused interventricular septum areas or findings indicative of interventricular septum ischemia were not observed during positive end-expiratory pressure.**

Conclusions: **The decrease in cardiac output during positive end-expiratory pressure is not caused by impaired interventricular septum blood supply. The preferential perfusion of the right ventricular interventricular septum indicates increased local right ventricular interventricular septum oxygen-demand and suggests that during positive end-expiratory pressure, this part of the interventricular septum functionally dissociates from the left ventricular interventricular septum and the left ventricular free wall to support the stressed right ventricle. (Crit Care Med 1991; 19:1414)**

KEY WORDS: **regional blood flow; hemodynamics; positive end-expiratory pressure; respiratory insufficiency; adult respiratory distress syndrome; microspheres; cardiac output; central venous pressure; ischemia**

"Paradoxic" systolic shifting of the interventricular septum toward the right ventricle with diastolic tamponade of the left ventricle is associated with a decrease in cardiac performance during ventilation with positive end-expiratory pressure (1–5). However, the mechanisms leading to paradoxic interventricular septum motion are not fully understood (6, 7).

While an inverse, negative end-diastolic left ventricle-to-right ventricle pressure gradient has been proposed as a possible causative factor (7–10), interventricular septum displacement has also been demonstrated in the presence of a positive left ventricle-to-right ventricle gradient (4, 11, 12). Hence, right ventricle dilation with subsequent reversal of the end-diastolic transseptal pressure gradient, despite being important, may not be the sole mechanism causing paradoxic interventricular septum shifting

From the Departments of Anesthesiology (Dr. Zwissler), and Surgical Research (Dr. Messmer), Klinikum Grosshadern, University of Munich, Munich; the Department of Experimental Surgery (Dr. Schosser, Ms. Schwickert, Mr. Spengler, Ms. Weiss, and Mr. Iber), Surgical Clinic, University of Heidelberg, Heidelberg, FRG.

Experiments were performed in the Department of Experimental Surgery, Surgical Clinic, University of Heidelberg, Heidelberg, FRG.

This study was supported, in part, by the German Research Council, Sonderforschungsbereich 320, Project C3.

Address requests for reprints to: Bernhard Zwissler, MD, Department of Surgical Research, University of Munich, Klinikum Grosshadern, Marchioninistrasse 15, D-8000, Munich, FRG.

Alternatively, interventricular septum shifting during positive end-expiratory pressure might be due to the fact that the interventricular septum builds part of the right ventricle cavity and, hence, lung injury and positive end-expiratory pressure impose an increased afterload to both the right ventricle free wall and the interventricular septum. Since a high afterload increases myocardial wall stress and oxygen consumption, positive end-expiratory pressure might result in ischemia of both the right ventricle free wall and the interventricular septum. Interventricular septum ischemia, in turn, impairs right ventricle function (16–20), and is associated with abnormal interventricular septum motion (16, 21, 22). Hence, abnormal interventricular septum perfusion or an adverse oxygen demand to interventricular septum perfusion relationship might also be present during positive end-expiratory pressure, thereby contributing to paradoxic interventricular septum motion, and decreased cardiac output. To test this hypothesis, we measured interventricular septum perfusion with high spatial resolution at three levels of positive end-expiratory pressure in a canine model of experimental ARDS. Thereby, we endeavored to assess the role of interventricular septum hypoperfusion as a causative factor of positive end-expiratory pressure-induced depression of cardiac output.

MATERIALS AND METHODS

Animal Preparation. The studies were performed in eight foxhounds of both sexes (17.7 ± 1.5 kg). All animals received care in compliance with the "Guide for the Care and Use of Laboratory Animals" (NIH publication No. 85–23, revised 1985). The institutional animal care and use committee approved this study.

After im premedication with 20 mg propiomazine (Combelen®, Bayer, Leverkusen, FRG), anesthesia was induced by iv injection of 20 mg/kg pentobarbital (Nembutal®, Ceva, Bad Segeberg, FRG), 0.75 mg/kg piritramide (Dipidolor®, Janssen, Neuss, FRG), and 0.25 mg/kg alcuronium (Alloferin®, Roche, Grenzach-Whylen, FRG), and anesthesia was maintained by iv infusion of these drugs (5, 0.15, 0.075 mg/kg·hr, respectively). Lactated Ringer's solution was administered iv at 5 mL/kg·hr. The dogs were endotracheally intubated and mechanically ventilated with 12 cycles/min and a tidal volume of 15 to 18 mL/kg using 100% oxygen (Servo® 900C, Siemens-Elema, Solna, Sweden).

Surgical Preparation. For monitoring of mean arterial (MAP) and central venous (CVP) pressures, catheters were inserted into the descending aorta and superior caval vein via the left brachial artery and vein, respectively. A pulmonary artery balloon flotation catheter (Swan-Ganz®, 7F, Edwards, Anasco, Puerto Rico) was inserted into the pulmonary artery via the right brachial vein for measurement of mean pulmonary artery pressure and cardiac output. A tip-manometer (PC 350, Millar Instruments, Houston, TX) was inserted into the right ventricle via the right external jugular vein for measurement of mean right ventricular, maximal right ventricular, and end-diastolic right ventricular pressures. A sidewinder catheter (6F, Cordis, Miami, FL) was passed via the right common carotid artery into the left atrium for injection of microspheres and measurement of mean left atrial pressure. The right femoral artery was cannulated for the withdrawal of the arterial reference sample. Intrathoracic pressure was estimated using a balloon catheter (National Catheter, NY) inserted into the esophagus and positioned at the level of the atrium. Subsequently, the dogs were turned to the left lateral decubitus position. In the lateral position, esophageal pressure reliably reflects intrathoracic pressure during positive end-expiratory pressure (23).

Experimental Protocol. Control measurements were performed 30 mins after surgical preparation. Thereafter, the lungs were embolized by right atrial injection of oleic acid (0.01 mL/kg) and repetitive doses of glass beads (mean diameter 100 μm) until mean pulmonary artery pressure had reached 35 to 40 mm Hg. This procedure provokes microvascular lung injury with pulmonary edema and a stable ARDS-like syndrome that is complicated by pulmonary hypertension (24). Accordingly, a decrease of pulmonary compliance and increases in intrapulmonary shunt, $Paco_2$, and deadspace ventilation were observed (unpublished data). In our model, mean pulmonary artery pressure decreased to approximately 30 mm Hg within 70 mins after embolization, but then remained unchanged for at least 80 mins (24). The second set of measurements (experimental ARDS) was obtained 70 mins after embolization.

End-expiratory pressure was increased stepwise to 10, 15, and 20 cm H_2O. During positive end-expiratory pressure, right ventricular end-diastolic pressure was kept constant by blood transfusions of 3.6 ± 2.1, 4.5 ± 2.4, and 4.5 ± 1.1 mL/kg (at positive end-expiratory pressures of 10, 15, and 20 cm H_2O, respectively). The measurements at the increased

positive end-expiratory pressures were performed, respectively, 10 mins after each vascular volume increase.

Measurements. Central hemodynamics (MAP, CVP, right venticular pressure, mean pulmonary artery pressure) and intrathoracic pressure were monitored on an eight-channel recorder (481, Gould-Brush, Cleveland, OH) and evaluated at end-expiration. The intrathoracic pressure was subtracted from CVP, mean left atrial pressure, mean pulmonary artery pressure, and right ventricular pressure to obtain transmural pressures. Thermodilution cardiac outputs were obtained in triplicate (SP 1435, Gould-Statham, Oxnard, CA).

The following variables were calculated: stroke volume = cardiac output × 1000/heart rate; pulmonary vascular resistance = (mean pulmonary artery pressure – mean left atrial pressure) × 79.9/cardiac output; right ventricular tension-time index = area beneath the systolic right ventricular pressure curve × heart rate; left ventricular tension-time index = area beneath the systolic aortic pressure curve × heart rate.

Microsphere Methodology. Interventricular septum perfusion was measured by the microsphere technique (25). Six distinctively radiolabeled microspheres (^{46}Sc, ^{95}Nb, ^{114}In, ^{51}Cr, ^{141}Ce, ^{103}Ru; NEN-TRAC®, DuPont, Wilmington, DE; 16.5-μm in diameter) were injected (≈480,000 microspheres/kg) in randomized order into the left atrium within 20 to 30 secs while a reference sample of blood was drawn (3.24 mL/min) from the abdominal aorta (Harvard Apparatus South Natick, MA). During collection of the reference sample, blood was substituted isovolemically to maintain hemodynamic stability (26).

Heart Dissection. The animals were killed by right atrial infusion of saturated potassium chloride prior to removal, fixation and dissection of the hearts. After fixation (6% formaldehyde, 1 wk), the atria were removed and the hearts were dissected into ten slices perpendicular to their axes (Fig. 1). Slices 1 through 8 were subdivided into left ventricular free wall, interventricular septum, and right ventricular free wall. Slices 9 and 10 were discarded. Each slice was cut into four (interventricular septum), six (left ventricular free wall) or, depending on the slice number, three to seven (right ventricular free wall) segments in anterior-posterior direction. Each segment was subdivided in transmural direction into three (right ventricular free wall) or four (interventricular septum, left ventricular free wall) layers of equal thickness. The total number of samples was 240 (weight, 239 ± 112 mg) in the left ventricular free wall and 126 (204 ± 70 mg) in the right ventricular free wall. Because of the irregular shape of the heart basis, "missing" samples occurred in the first slice, resulting in a variable number of 124 to 127 interventricular septum tissue samples (152 ± 52 mg).

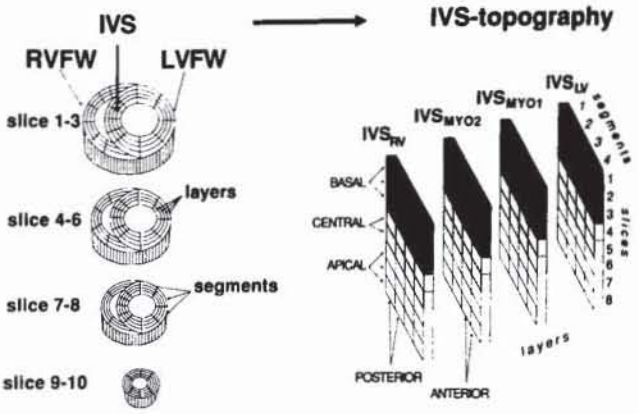

Figure 1. Heart dissection scheme. *Left panel,* the hierarchic structure of the heart dissection scheme. The hearts were cut into slices; the right and left ventricular free wall (*RVFW, LVFW*), and the interventricular septum (*IVS*) were separated and further subdivided into layers and segments. *Right panel,* the way interventricular septum tissue flow was summarized for parts of the analyses according to their location. IVS_{RV}, right ventricular part of the interventricular septum; IVS_{MYO2}, myocardial 2 section of the interventricular septum; IVS_{MYO1}, myocardial 1 section of the interventricular septum; IVS_{LV}, left ventricular section of the interventricular septum.

For parts of the analyses, samples were categorized according to their topographic location (Fig. 1). Interventricular septum regions termed left ventricular interventricular septum, myocardial 1 interventricular septum, myocardial 2 interventricular septum, and right ventricular interventricular septum comprised samples from the left ventricular-subendocardial, midmyocardial, and right ventricular-subendocardial layers of the interventricular septum, respectively. Corresponding layers of the left ventricular free wall were termed left ventricular subendocardium, left ventricular myocardial 1, left ventricular myocardial 2, and left ventricular subepicardium. Regions termed basal, central, and apical included interventricular septum samples from slices 1 through 3, 4 through 5, and 6 through 8, respectively. Regions termed anterior and posterior included interventricular septum samples from the segments 1 through 2 and 3 through 4, respectively.

Assessment of Regional Blood Flow. The radioactivities of both the tissue and reference samples were counted (Auto-Gamma 5220, Packard Instruments, Downers Grove, IL) and sample blood

flow was calculated as $Q_{sample} = Q_{ar} \times I_{sample}/I_{ar}$ (mL/min), where Q_{ar} is the rate of withdrawal of arterial reference blood (mL/min), I_{ar} are counts/min in arterial reference blood, and I_{sample} are counts/min in the tissue sample. Sample flow then was normalized to 1 g. The spatial heterogeneity of interventricular septum flow was calculated as the relative dispersion (SD/mean × 100) of interventricular septum flow values.

Validation of the Microsphere Method. A total of approximately 1.1×10^6 microspheres per experiment were trapped within the interventricular septum. Based on 6×10^6 capillaries per gram of myocardial tissue (27) and a mean interventricular septum weight of 20 g, the fraction of capillaries blocked by microspheres was <1% in our experiments, thereby excluding major alterations of interventricular septum microcirculation due to microsphere injection (27).

In two dogs, the methodologic error of the microsphere technique was assessed by simultaneous injection of five different isotopes. The errors amounted to 5.1% and 8.7%, respectively, in these two experiments and were similar to those found by others for the heart (28, 29).

In six dogs, myocardial shunt flow was assessed by quantifying the number of particles appearing in coronary sinus blood subsequent to microsphere injection. Myocardial shunt flow was 1.4 ± 1.0% of total myocardial blood flow with no differences at the five timepoints of measurement. Therefore, myocardial shunt flow was neglected for calculation of nutritive interventricular septum flow.

Fluid Management. Absolute hypovolemia due to arterial reference sampling and relative hypovolemia during positive end-expiratory pressure was prevented by volume substitution. Blood rather than colloids was used to maintain a stable hematocrit and hemoglobin concentration throughout the study, and was obtained by two means: an average of 200 mL of blood was received by isovolemically hemodiluting the animals with 6% dextran 60 (Macrodex® 6%, Schiwa, Glandorf, FRG) to a hematocrit of 28% before the onset of the experiment. Additionally, 400 to 500 mL of blood was obtained from an awake, premedicated donor dog on the day of experiment. Blood from both sources was mixed (hematocrit 28 ± 2%) and the mixture was used for volume substitution.

Statistical Analyses. Data are presented as mean ± SD. Student's paired *t*-test and Bonferroni correction were used to assess both the changes in hemodynamics and tissue perfusion between different measurements (experimental ARDS vs. control, 20 cm H_2O positive end-expiratory pressure vs. experimental ARDS, and 20 cm H_2O positive end-expiratory pressure vs. control), as well as to compare tissue perfusion between different regions at a given time point of measurement. The latter use of the paired *t*-test seems justified, since different regions of the heart share a common coronary vasculature and, hence, flow values are dependent. Differences were considered significant at $p < .05$.

RESULTS

Central Hemodynamics. As shown in Table 1, experimental ARDS was characterized by significant increases in heart rate, mean pulmonary artery pressure, pulmonary vascular resistance, mean right ventricular pressure, maximal right ventricular pressure, right ventricular tension-time index, and right ventricular dP/dt_{max}. Despite a 39% decrease of stroke volume ($p < .05$), cardiac output and mean arterial pressure were unchanged. Positive end-expiratory pressure of 20 cm H_2O caused further increases in pulmonary vascular resistance (+61%, $p < .01$) and right ventricular tension-time index (+35%, $p < .01$), and decreases in cardiac output (–25%, $p < .01$) and stroke volume (–41%, $p < .001$).

Total Interventricular Septum Perfusion. Total interventricular blood flow was not significantly affected by experimental ARDS or positive end-expiratory pressure (Fig. 2), while interventricular septum blood flow relative to cardiac output increased from 0.56% to 0.73% in experimental ARDS ($p < .001$), and to 1.0% during positive end-expiratory pressure of 20 cm H_2O ($p < .001$, Fig. 2).

Relative Frequency of Interventricular Septum Flow Values (Histograms). The interventricular septum flow histograms demonstrated a unimodal distribution of flow during positive end-expiratory pressure (Fig. 3). At control, 7% to 8% of all tissue samples had a flow of <0.5 mL/min·g, while this percentage decreased to 2.5% during experimental ARDS, and to 1% during positive end-expiratory pressure of 20 cm H_2O. During positive end-expiratory pressure, none of the tissue samples had a flow <0.3 mL/min·g.

Regional Interventricular Septum Perfusion (Color-Coded Display). To visualize the pattern of interventricular septum perfusion, pseudocolors were attributed to sample flow value (red, high flow; blue, low flow) and are displayed in Figure 4. There was a flow gradient between left ventricular interventricular septum (high flow) and right ventricular interventricular septum (low flow) at control, an increase

Table 1. Cardiovascular response to experimental adult respiratory distress syndrome (ARDS) and positive end-expiratory pressure (mean ± SD values)

			Positive End-Expiratory Pressure		
	Control	ARDS	10 cm H_2O	15 cm H_2O	20 cm H_2O
HR (beats/min)	72 ± 19	107 ± 17[b]	99 ± 16	109 ± 19	124 ± 10[f]
Cardiac output (L/min)	3.1 ± 0.7	2.8 ± 0.8	2.5 ± 0.7	2.4 ± 0.6	2.1 ± 0.6[b,d]
SV (mL)	44 ± 13	27 ± 8[a]	25 ± 6	22 ± 5	16 ± 6[c,e]
MAP (mm Hg)	102 ± 9	102 ± 8	108 ± 13	111 ± 17	102 ± 13
MLAP (mm Hg)	4.5 ± 3.3	2.6 ± 2.5	2.8 ± 1.9	2.3 ± 1.9	1.8 ± 2.1
MPAP (mm Hg)	11 ± 3	32 ± 5[c]	31 ± 4	32 ± 3	37 ± 3[a,f]
MRVP (mm Hg)	6 ± 2	16 ± 3[c]	15 ± 3	15 ± 2	17 ± 2[f]
RVP_{max} (mm Hg)	20 ± 3	41 ± 8[c]	38 ± 5	38 ± 4	41 ± 2[f]
RVEDP (mm Hg)	1.3 ± 2.5	2.2 ± 2.8	3.0 ± 2.6	1.6 ± 2.0	1.0 ± 1.0
CVP (mm Hg)	0.5 ± 1.8	1.3 ± 1.4	1.1 ± 0.9	1.0 ± 1.7	0.8 ± 1.4
RV dP/dt_{max} (mm Hg/sec)	370 ± 92	589 ± 174[b]	505 ± 136	536 ± 136	567 ± 66[e]
PVR (dyne·sec/cm^5)	156 ± 81	907 ± 350[c]	947 ± 321	1081 ± 378	1,461 ± 549[b,f]
RV tension-time index (mm Hg·sec/min)	274 ± 56	745 ± 129[c]	742 ± 139	868 ± 93	1007 ± 71[b,f]
LV tension-time index (mm Hg·sec/min)	2186 ± 578	2734 ± 325	2793 ± 280	3164 ± 519	3076 ± 311[d]

[a] $p < .05$; [b] $p < .01$; [c] $p < .001$ ARDS vs. control, and PEEP 20 cm H_2O vs. ARDS.
[d] $p < .05$; [e] $p < .01$; [f] $p < .001$ PEEP 20 cm H_2O vs. control.

HR, heart rate; SV, stroke volume; MAP, mean arterial pressure; MLAP, mean left atrial pressure; MPAP, mean pulmonary artery pressure; RV, right ventricular; MRVP, mean RV pressure; RVP_{max}, maximal RV pressure; RVEDP, RV end-diastolic pressure; CVP, central venous pressure; RV dP/dt_{max}, maximal rate of RV pressure increase; PVR, pulmonary vascular resistance; LV, left ventricular.

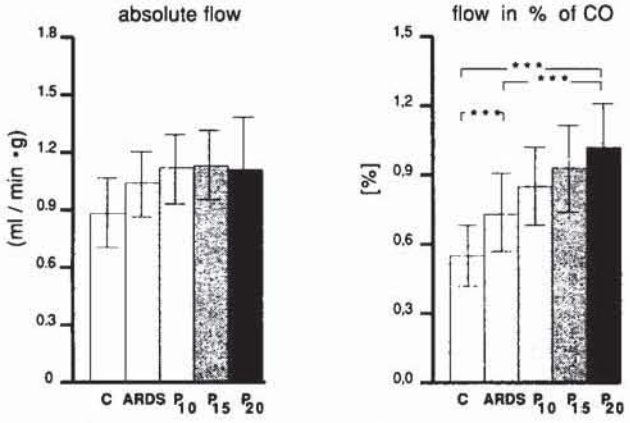

Figure 2. Interventricular septum blood flow during experimental adult respiratory distress syndrome (*ARDS*) and positive end-expiratory pressure. Absolute (*left panel*) and relative (in % of cardiac output) interventricular septum blood flow are depicted at control (*C*), induction of ARDS, and at positive end-expiratory pressures of 10 (P_{10}), 15 (P_{15}), and 20 (P_{20}) cm H_2O (mean ± SD, n = 8). ***$p < .001$. Data are mean ± SD.

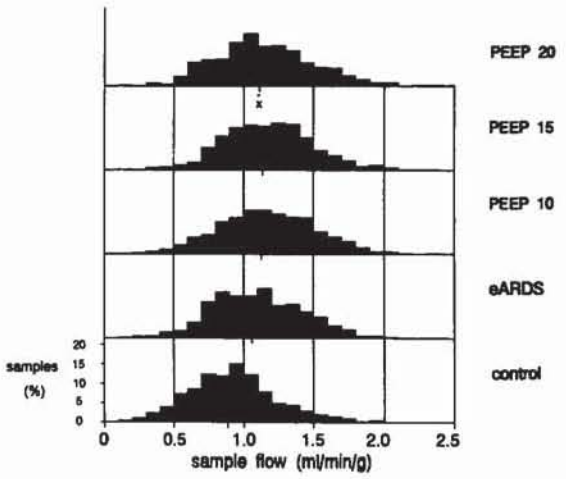

Figure 3. Distribution of interventricular septum flow values. Blood flow values, as obtained in each single interventricular septum sample of eight experiments (n = 994), were displayed in a histogram. During experimental ARDS (*eARDS*) and positive end-expiratory pressure (*PEEP*, cm H_2O), a shift of the histogram to the right was observed, indicating uncompromised tissue perfusion at all time points of measurement. The vertical axis in this histogram (samples %) describes the percentage (100% = all samples included in the histogram at each point of measurement) of tissue samples having a certain blood flow as indicated on the horizontal axis.

of right ventricular interventricular septum flow during experimental ARDS, and a reversal of the left ventricular/right ventricular interventricular septum flow gradient during positive end-expiratory pressure of 20 cm H_2O. At control, spatial heterogeneity of flow was obvious within each layer of the interventricular septum, while flow became more uniform during experimental ARDS and

positive end-expiratory pressure. Flow during positive end-expiratory pressure of 20 cm H_2O exceeded the control values in all samples. The decreased scatter of flow was reflected by a decrease of the spatial heterogeneity of interventricular septum flow (expressed as the relative dispersion of sample flow values) from 30.3% at control to 23.7% during experimental ARDS ($p < .001$), with no change during positive end-expiratory pressure. Within single interventricular septum layers, the spatial heterogeneity of interventricular septum flow ranged from 22.4% to 28.0% at control and was 17.6% to 23.4% at positive end-expiratory pressure of 20 cm H_2O.

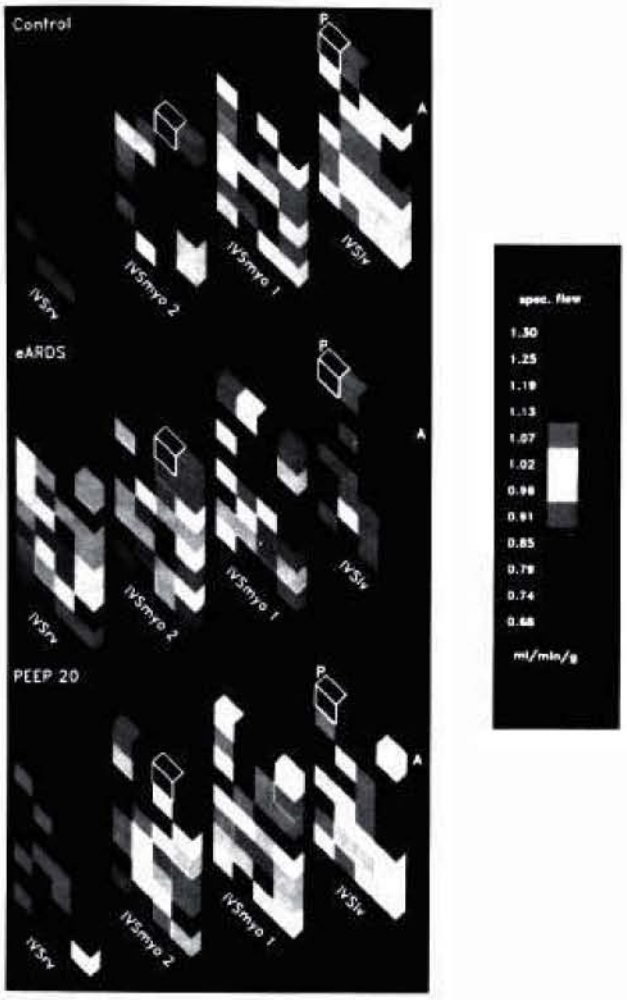

Figure 4. Influence of experimental ARDS (*eARDS*) and positive end-expiratory pressure (*PEEP*) on regional interventricular septum (*IVS*) perfusion (pseudocolor display). To visualize changes of regional blood flow within the interventricular septum, pseudocolors were attributed to mean sample flow values normalized to 1 g of tissue weight (= specific or "spec." flow) from eight experiments at control, experimental ARDS, and positive end-expiratory pressure of 20 cm H_2O (*PEEP 20*), and were included into the scheme of the interventricular septum depicted in Figure 1. *IVSrv*, right ventricular part of the interventricular septum; *IVSmyo1 and IVSmyo2*, midmyocardial parts of the interventricular septum; *IVSlv*, left ventricular part of the interventricular septum; *P*, posterior, *A*, anterior. Because of the irregular shape of the heart basis, no samples could be obtained from two locations of slice 1. In the scheme, these 'samples' were indicated by black color confined by a white margin. The figure demonstrates the elimination of the left ventricular/right ventricular interventricular septum flow gradient by experimental ARDS and a reversal of this gradient at positive end-expiratory pressure of 20 cm H_2O.

Regional Interventricular Septum Perfusion (Quantitative Analysis). Posterior exceeded anterior interventricular septum flow at control ($p < .05$), but did not differ during experimental ARDS or positive end-expiratory pressure (Fig. 5). Apical exceeded basal interventricular septum flow at control ($p < .01$), thereby abolishing the basal/apical gradient (Fig. 5).

At control, a transseptal flow gradient was present (Fig. 5). While flow was 1.03 ± 0.25 mL/min·g in the left ventricular interventricular septum, it was 0.69 ± 0.19 mL/min·g in the right ventricular interventricular septum. Experimental ARDS caused a 40% increase of blood supply to the right ventricular interventricular septum ($p < .05$), without affecting myocardial 1 interventricular septum, myocardial 2 interventricular septum, or left ventricular

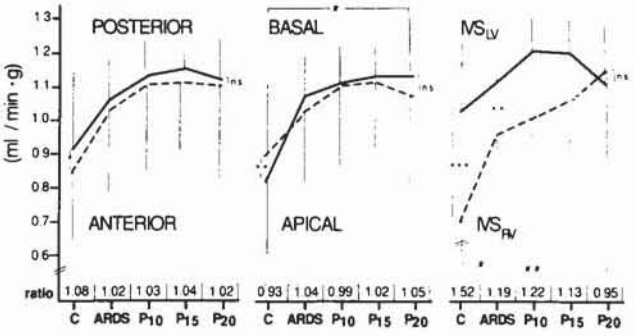

Figure 5. Influence of experimental adult respiratory distress syndrome (*ARDS*) and positive end-expiratory pressure on regional interventricular septum (*IVS*) perfusion (quantitative analysis). Several regions of the interventricular septum (posterior, basal, left ventricular part of the interventricular septum; anterior, apical, and right ventricular part of the interventricular septum) were analyzed with respect to the influence of experimental ARDS and positive end-expiratory pressure of 20 cm H_2O on a) absolute changes of blood flow within each region ($^*p < .05$, $^{**}p < .01$) and on b) the flow gradient (ratio) between different regions ($^*p < .05$, $^{**}p < .01$). Data are mean ± SD of eight experiments. Blood flow of the central interventricular septum (not included in the figure) was 0.90 ± 0.20 mL/min·g (control), 1.04 ± 0.25 (experimental ARDS), 1.13 ± 0.24 (positive end-expiratory pressure of 10 cm H_2O [P_{10}]), 1.14 ± 0.22 (positive end-expiratory pressure of 15 cm H_2O [P_{15}]), and 1.12 ± 0.28 (positive end-expiratory pressure of 20 cm H_2O [P_{20}]), respectively.

interventricular septum. The left ventricular/right ventricular interventricular septum flow ratio decreased to 1.19 ± 0.18 ($p < .001$). Positive end-expiratory pressure of 20 cm H_2O further increased blood flow to the right ventricular interventricular septum flow (+68%, $p < .01$), but decreased the left ventricular/right ventricular interventricular septum flow ratio to 0.95 ± 0.10 ($p < .001$).

Interventricular Septum Perfusion as Compared With the Left Ventricular and Right Ventricular Free Walls. In Figure 6, myocardial blood flow is visualized using color-coding. Compared with control, there was a gradual redistribution of flow in favor of the right ventricular part of the interventricular septum during experimental ARDS and positive end-expiratory pressures at 10 and 20 cm H_2O, while perfusion of the corresponding layers of the left ventricular free wall remained basically unchanged. Within the right ventricular free wall, experimental ARDS and positive end-expiratory pressure resulted in an increase of flow toward all right ventricular layers.

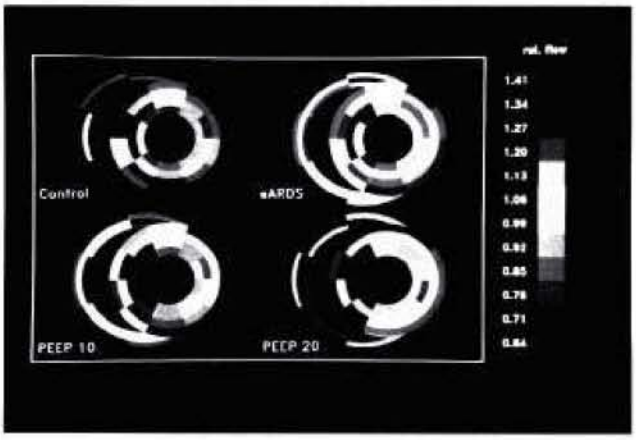

Figure 6. Influence of experimental ARDS (*eARDS*) and positive end-expiratory pressure (*PEEP 10*, 10 cm H_2O and *PEEP 20*, 20 cm H_2O) on regional interventricular septum perfusion as compared with the left ventricular and right ventricular free walls (qualitative analysis). The influence of experimental ARDS and positive end-expiratory pressure on myocardial blood flow distribution is depicted for slice 4 (for topography, see Fig. 1, *left panel*) of a representative experiment (no. 6). Since absolute perfusion differs considerably between the right and the left heart, relative flow values are shown and were obtained as follows: mean tissue flow of the four time points of measurement (control, experimental ARDS, positive end-expiratory pressures of 10 [*PEEP 10*] and 20 [*PEEP 20*] cm H_2O) was calculated separately for the right ventricular free wall and the left ventricular free wall plus interventricular septum, and individual right ventricular free wall or left ventricular free wall plus interventricular septum sample flow was then related to these mean values. A relative flow (*right panel*) value of 1.0 means that individual sample flow equaled mean flow within the respective part of the heart; samples with a relative flow >1.0 exceeded mean flow and vice versa. This technique allows analysis of changes of blood flow distribution within both the right ventricular free wall and the left ventricular free wall/interventricular septum using the same scale despite differences in absolute blood flow. Compared with control state (*upper left*), there was a gradual redistribution of blood flow in favor of the right ventricular part of the interventricular septum during experimental ARDS (*upper right*), positive end-expiratory pressure of 10 (*lower left*), and 20 (*lower right*) cm H_2O, while perfusion of the corresponding layers of the left ventricular free wall remained basically unchanged. Within the free wall, experimental ARDS and positive end-expiratory pressure resulted in a marked increase of flow toward all right ventricular layers.

Flow values within interventricular and left ventricular free wall layers are illustrated in Figure 7. At control, flow was higher within the interventricular septum than flow within the corresponding layers of the left ventricular free wall, the difference being significant between left ventricular interventricular septum and left ventricular subendocardium ($p < .05$). During experimental ARDS and positive end-expiratory pressure, the relation of flow between interventricular septum and left ventricular free wall was unchanged in those layers confining the left ventricular lumen (left ventricular interventricular septum, myocardial 1 interventricular septum and left ventricular subendocardium, left ventricular myocardial 1, respectively), while it increased in the "outer" layers ($p < .01$ at positive end-expiratory pressure of 20 cm H_2O). The increase of flow within myocardial 2 and right ventricular interventricular

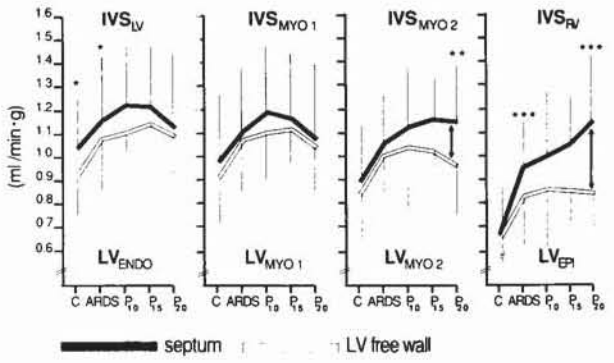

Figure 7. Influence of experimental adult respiratory distress syndrome (ARDS) and positive end-expiratory pressure on regional interventricular septum perfusion as compared with the left ventricular (*LV*) free wall (quantitative analysis). Tissue perfusion was quantified in the four layers of the interventricular septum (left ventricular [IVS_{LV}], myocardial layer 1 [IVS_{MYO1}], myocardial layer 2 [IVS_{MYO2}], and right ventricular [IVS_{RV}]) and was compared with perfusion within the corresponding four layers of the left ventricular free wall (left ventricular subendocardium [LV_{ENDO}], left ventricular myocardial layer 1 [LV_{MYO1}], myocardial layer 2 [LV_{MYO2}], and left ventricular subepicardium [LV_{EPI}]) at control, experimental ARDS, and positive end-expiratory pressure of 20 cm H_2O (mean ± SD of eight experiments). *Arrows*, dissociation of blood flow. $^{*}p < .05$; $^{**}p < .01$; $^{***}p < .001$ indicate septum vs. left ventricular free wall.

septum paralleled right ventricular free wall flow, which increased from 0.48 ± 0.13 (control) to 0.81 ± 0.21 (experimental ARDS, $p < .01$), and 0.92 ± 0.22 mL/min·g at positive end-expiratory pressure of 20 cm H_2O.

DISCUSSION

Data on interventricular septum perfusion during positive end-expiratory pressure are limited (30–33) and were obtained under experimental conditions distinctly different from the clinical situation (31–33). Most often, analyses were restricted to changes of average interventricular septum blood flow (30–32). In contrast, we examined both average and regional interventricular septum perfusion in a model closely simulating the clinical setting since a) all measurements were performed in dogs with closed pericardium and chest, b) a stable ARDS-like syndrome was present (24), and c) volume was substituted during positive end-expiratory pressure.

Total Blood Flow. We found that positive end-expiratory pressure of 20 cm H_2O did not compromise absolute interventricular septum flow, but increased relative septal flow. In contrast, a decrease of absolute interventricular septum perfusion and a redistribution of systemic blood flow to the disadvantage of the interventricular septum have been reported (31, 33). Differences in experimental set-up may explain part of these discrepant findings. Although the studies were performed in anesthetized dogs, heart rate under control conditions was 85 beats/min in the present experiments, but was 165 and 187 beats/min in those latter studies, suggesting different levels of anesthesia. Accordingly, baseline values of absolute interventricular septum perfusion were extremely high (1.67 to 2.16 mL/min·g) in the studies of Jacobs and Venus (31, 33), whereas much lower values (0.85 to 1.30 mL/min·g) were found by others (32, 34) and ourselves. Since sympathetic nervous system activation may reduce myocardial vasodilator reserve (34), we speculate that interventricular septum perfusion decreased in the experiments of Jacobs and Venus, because the interventricular septum (due to compromised flow reserve) failed to compensate for the positive end-expiratory pressure-induced reduction of cardiac output.

Similar to the present experiments, relative interventricular septal flow increased subsequent to positive end-expiratory pressure in dogs with moderate heart rate and lower interventricular septal perfusion at control (30, 32). However, this redistribution of flow in favor of the interventricular septum did not prevent the decrease of absolute interventricular septal flow in the studies of Manny et al. (32) (nonvolume-substituted dogs) and Beyer and Messmer (30) (series 1: dogs with lung injury, volume-substituted). On the other hand, interventricular septal perfusion was preserved in the present experiments and those studies of Beyer and Messmer (30) (series 2: dogs without lung injury, volume-substituted).

Independent from the relative importance of factors like anesthesia, volume management, and status of the lungs in the modulation of interventricular septum blood flow, our study provides strong evidence of a redistribution of cardiac output in favor of the interventricular septum at unchanged or even reduced right ventricular and left ventricular coronary artery driving pressures. This finding indicates unrestricted interventricular septum vasodilator reserve and suggests that positive end-expiratory pressure does not induce global interventricular septum ischemia under experimental conditions similar to the condition of ARDS patients.

Regional Blood Flow. The main goal of the present study was the "high-resolution" analysis of interventricular septum blood flow during positive end-expiratory pressure. Data on this topic have not been published. Previously, average interventricular septum perfusion was derived from 5 to 15 "representative" tissue samples (31, 33), and neither the number nor the localization of samples examined was indicated in other studies (30, 32). However, such analyses neglect the consideration that the interventricular septum is not uniform with respect to ontogenesis, blood supply, location of maximum motion, and response to ischemia (3, 35–37). Hence, a complete dissection of the interventricular septum into multiple tissue samples was performed to characterize interventricular septal flow distribution.

Interventricular Septum Versus Left Ventricular Free Wall Flow (Flow Across Layers). At control, flow gradients similar to those gradients described previously were found across the layers of the interventricular septum and the left ventricular free wall (33, 34, 38). In contrast, flow gradients were absent between corresponding layers of the interventricular septum and left ventricular free wall, supporting the view that the interventricular septum represents a functional part of the left ventricle (39).

During experimental ARDS and positive end-expiratory pressure, blood flow changed nonuniformly. In the right ventricular interventricular septum, similar to the right ventricular free wall, blood flow increased in parallel with an increase of pulmonary vascular resistance, maximum right ventricular

pressure, and right ventricular tension-time index. This finding indicates an increased local oxygen demand, which could be explained by the fact that the interventricular septum builds part of the right ventricular cavity. One might imagine that, at an increased right ventricular afterload, the right-sided interventricular septal fibers (similar to right ventricular free wall fibers) start to contract more vigorously, thereby causing interventricular septal thickening and bulging toward the right ventricular free wall, which could support right ventricular ejection. In contrast to the right ventricular interventricular septum and right ventricular free wall, flow to the left ventricular interventricular septum and left ventricular free wall did not change noticeably, suggesting that the left ventricular interventricular septum and left ventricular free wall were not functionally affected by the increase of right ventricular afterload.

These data indicate that a dissociation of interventricular septum blood flow occurs during experimental ARDS and positive end-expiratory pressure, which most likely is caused by a functional dissociation of the right ventricular and left ventricular part of the interventricular septum because of different loading conditions in both ventricles.

Since it is difficult to assess the interventricular septal oxygen demand in an in vivo model, we could not exclude that relative hypoperfusion of the left ventricular or right ventricular interventricular septum might have been present in our experiments. Yet, no decrease of the subendo-subepicardial (left ventricular/right ventricular interventricular septum) flow ratio below 0.7 to 0.8 (40–42) has been observed. With respect to right ventricular interventricular septum, the 68% increase of blood flow might not have been sufficient to compensate for the increased oxygen demand as estimated by the threefold increase of right ventricular tension time index at positive end-expiratory pressure of 20 cm H_2O. However, right ventricular interventricular septum perfusion during positive end-expiratory pressure of 20 cm H_2O could be further increased (+21%) by administration of norepinephrine despite unchanged right ventricular driving pressure (data not shown). This finding suggests unexhausted right ventricular interventricular septum vasodilator reserve during positive end-expiratory pressure of 20 cm H_2O.

Anterior Versus Posterior Interventricular Septum Flow. Anterior and posterior interventricular septum differ with respect to embryologic origin and blood supply (3, 35). However, our finding of a uniform response of interventricular septal flow to experimental ARDS and positive end-expiratory pressure suggests that a selective hypoperfusion of anterior or posterior interventricular septum did not occur under these conditions.

Basal Versus Apical Interventricular Septum Flow. Since abnormal interventricular septum displacement subsequent to right ventricular volume loading occurs predominantly in the basal part (37), interventricular septum perfusion was examined for the occurrence of an apical-to-basal flow gradient. Such gradient was not found, except at control. This observation suggests that paradoxic shifting of the interventricular septum during positive end-expiratory pressure, if localized in the basal interventricular septum, is not likely to be caused by hypoperfusion of basal interventricular septum.

Perfusion of Single Interventricular Septum Tissue Samples. During hypoxia, the distribution of coronary artery blood flow becomes heterogeneous, resulting in small, but visible zones of anoxic myocardial tissue which is surrounded by normoxic tissue (43). Accordingly, blood flow rates of <0.15 mL/min·g were reported together with normal flow in ischemic left ventricular tissue, resulting in a bimodal flow histogram and an increase of spatial flow heterogeneity (42). In contrast, in our study: a) the shape of the interventricular septum flow histogram was unimodal at control with no change during positive end-expiratory pressure; b) samples with a blood flow of <0.3 mL/min·g were absent; and c) relative flow dispersion decreased from 30.3% at control to 23.7% during positive end-expiratory pressure of 20 cm H_2O.

In summary, there was no experimental evidence of critical hypoperfusion within any region of the interventricular septum subsequent to the initiation of positive end-expiratory pressure. Therefore, we conclude that interventricular septum ischemia is not likely to contribute to paradoxic interventricular septum shifting and circulatory depression during positive end-expiratory pressure. Furthermore, our data demonstrated that a high right ventricular afterload affects blood flow in the interventricular septum and the left ventricular free wall differently. The preferential perfusion of the right ventricular part of the interventricular septum therefore indicates an increase of local oxygen demand and suggests that these interventricular septal regions have functionally dissociated from the left ventricle to support the stressed right ventricle.

ACKNOWLEDGMENTS

The authors thank Mrs. R. Schwarz, J. Schulte, K. Sonnenberg, H. Voigt and G. Rothkegel for their technical assistance.

REFERENCES

1. Laver MB, Strauss HW, Pohost GM: Right and left ventricular geometry: Adjustments during acute respiratory failure. *Crit Care Med* 1979; 7:509
2. Jardin F, Farcot JC, Boisante L, et al: Influence of positive end-expiratory pressure on left ventricular performance. *N Engl J Med* 1981; 304:387
3. Kaul S: The interventricular septum in health and disease. *Am Heart J* 1986; 112:568
4. Forst H, Racenberg J, Peter K, et al: Right ventricular performance and positive end-expiratory pressure ventilation. *In:* Shock and the Adult Respiratory Distress Syndrome. Kox W, Bihari D (Eds). Berlin, Heidelberg, New York, Springer Verlag, 1987, pp 123–136
5. Forst H, Zwissler B, Racenberg J, et al: "Paradoxic" septal motion during positive end-expiratory pressure ventilation. *In*: Interaction Between Heart and Lung. Daum S (Ed). Stuttgart, New York, Georg Thieme Verlag, 1989, pp 34–36
6. Guzman PA, Maughan WL, Yin FC, et al: Transseptal pressure gradient with leftward septal displacement during the Mueller manoeuvre in man. *Br Heart J* 1981; 46:657
7. Kingma I, Tyberg JV, Smith ER: Effects of diastolic transseptal pressure gradient on ventricular septal position and motion. *Circulation* 1983; 68:1304
8. Tanaka H, Tei C, Nakao S, et al: Diastolic bulging of the interventricular septum toward the left ventricle. An echocardiographic manifestation of negative interventricular pressure gradient between left and right ventricles during diastole. *Circulation* 1980; 62:558
9. Brinker JA, Weiss JL, Lappe DL, et al: Leftward septal displacement during right ventricular loading in man. *Circulation* 1980; 61:626
10. Feneley M, Gavaghan T: Paradoxical and pseudoparadoxical interventricular septal motion in patients with right ventricular volume overload. *Circulation* 1986; 2:230
11. Agata Y, Hiraishi S, Misawa H, et al: Two-dimensional echocardiographic determinants of interventricular septal configurations in right or left ventricular overload. *Am Heart J* 1985; 110:819
12. Molaug M, Geiran O, Stokland O, et al: Dynamics of the interventricular septum and free ventricular walls during blood volume expansion and selective right ventricular volume loading in dogs. *Acta Physiol Scand* 1982; 116:245
13. Louie EK, Rich S, Brundage BH: Doppler echocardiographic assessment of impaired left ventricular filling in patients with right ventricular pressure overload due to primary pulmonary hypertension. *J Am Coll Cardiol* 1986; 8:1298
14. Visner MS, Arentzen CE, O'Connor MJ, et al: Alterations in left ventricular three-dimensional dynamic geometry and systolic function during acute right ventricular hypertension in the conscious dog. *Circulation* 1983; 67:353
15. Kent RS, Carew TE, LeWinter MM, et al: Comparison of left ventricular free wall and septal diastolic compliance in the dog. *Am J Physiol* 1978; 234:392
16. Agarwal JB, Yamazaki H, Bodenheimer MM, et al: Effects of isolated interventricular septal ischemia on global and segmental function of the canine right and left ventricle. *Am Heart J* 1981; 102:654
17. Isner JM, Roberts WC: Right ventricular infarction complicating left ventricular infarction secondary to coronary heart disease. Frequency, location, associated findings and significance from analysis of 236 necropsy patients with acute or healed myocardial infarction. *Am J Cardiol* 1978; 42:885
18. Brooks H, Holland R, Al-Sadir J: Right ventricular performance during ischemia: An anatomic and hemodynamic analysis. *Am J Physiol* 1977; 233:505
19. Fixler DE, Monroe GA, Wheeler JM: Hemodynamic alterations during septal or right ventricular ischemia in dogs. *Am Heart J* 1977; 93:210
20. Tani M: Roles of the right ventricular free wall and ventricular septum in right ventricular performance and influence of the parietal pericardium during right ventricular failure in dogs. *Am J Cardiol* 1983; 52:196
21. Kerber RE, Marcus ML, Wilson R, et al: Effects of acute coronary occlusion on the motion and perfusion of the normal and ischemic interventricular septum. *Circulation* 1976; 54:928
22. Kolibash AJ, Beaver BM, Fulkerson PK, et al: The relationship between abnormal echocardiographic septal motion and myocardial perfusion in patients with significant obstruction of the left anterior descending artery. *Circulation* 1977; 56:780
23. Craven KD, Wood LDH: Extrapericardial and esophageal pressures with positive end-expiratory pressure in dogs. *J Appl Physiol* 1981; 51:798
24. Zwissler B, Forst H, Ishii K, et al: A new experimental model of ARDS and pulmonary hypertension in the dog. *Res Exp Med* 1989; 189:427
25. Heyman MA, Payne BD, Hoffman IE, et al: Blood flow measurements with radionuclide-labeled particles. *Prog Cardiovasc Dis* 1977; 20:55
26. von Ritter C, Hinder RA, Womack W, et al: Microsphere estimates of blood flow: Methodological considerations. *Am J Physiol* 1988; 254:G275
27. Yipintsoi T, Dobbs WA Jr, Scanlon PD, et al: Regional distribution of diffusible tracers and carbonized microspheres in the left ventricle of the isolated heart. *Circ Res* 1973; 33:573
28. King RB, Bassingthwaighte JB, Hales JRS, et al: Stability of heterogeneity of myocardial blood flow in normal awake baboons. *Circ Res* 1985; 57:285
29. Franzen D, Conway RS, Zhang H, et al: Spatial heterogeneity of local blood flow and metabolite content in dog hearts. *Am J Physiol* 1988; 254:344
30. Beyer J, Messmer K: Organdurchblutung und Sauerstoffversorgung bei PEEP. (Anaesthesiol. u. Intensivmed. 145). Berlin, Heidelberg, New York, Springer Verlag, 1982
31. Jacobs HK, Venus B: Left ventricular regional myocardial blood flows during controlled positive pressure ventilation and positive end-expiratory pressure in dogs. *Crit Care Med* 1983; 11:872
32. Manny J, Justice R, Hechtman HB: Abnormalities in organ blood flow and its distribution during positive end-expiratory pressure. *Surgery* 1979; 85:425
33. Venus B, Jacobs HK: Alterations in regional myocardial blood flows during different levels of positive end-expiratory pressure. *Crit Care Med* 1984; 12:96
34. Parks C, Manohar M, Lundeen G: Regional myocardial blood flow and coronary vascular reserve in unanesthetized ponies during pacing-induced ventricular tachycardia. *J Surg Res* 1983; 35:119
35. Nakamura M, Sasayama S, Takahashi M, et al: Regional dysfunction of the interventricular septum during acute coronary artery occlusion. *Cardiovasc Res* 1982; 16:144
36. Sostman HD, Kelley MJ, Langou RA: Perfusion of the canine interventricular septum: Significance of right coronary artery supply. *Am Heart J* 1977; 94:611
37. Weyman AE, Wann S, Feigenbaum H, et al: Mechanism of abnormal septal motion in patients with right ventricular volume overload. *Circulation* 1976; 54:179

38. Manohar M: Transmural coronary vasodilator reserve, and flow distribution during tachycardia in conscious young swine with right ventricular hypertrophy. *Cardiovasc Res* 1985; 19:104
39. Banka VS, Agarwal JB, Bodenheimer MM, et al: Interventricular septal motion: Biventricular angiographic assessment of its relative contribution to left and right ventricular contraction. *Circulation* 1981; 64:992
40. Domenech RJ, Hoffman JE, Noble MM, et al: Total and regional coronary blood flow measured by radioactive microspheres in conscious and anesthetized dogs. *Circ Res* 1969; 25:581
41. Utley J, Carlson EL, Hoffman JIE, et al: Total and regional myocardial blood flow measurements with 25μ, 15μ, 9μ and filtered 1-10μ diameter microspheres and antipyrine in dogs and sheep. *Circ Res* 1974; 34:391
42. Marcus ML, Kerber RE, Ehrhardt J, et al: Three dimensional geometry of acutely ischemic myocardium. *Circulation* 1975; 52:254
43. Steenbergen C, Deleeuw G, Barlow C, et al: Heterogeneity of the hypoxic state in perfused rat heart. *Circ Res* 1977; 41:606